Development and Evaluation of 6-Component Load Cell for Land-Based Test of Helicopter Rotor Dynamics

Jong-Ryeol Noh and Jae-Young JEON
R &D Center, POWER MnC Co., Ltd., Taejon, Korea

ABSTRACT

A 6-component force transducer was developed and evaluated for small-scale model test of helicopter rotor dynamics. The evaluation of the transducer was done mainly through interference check using multi-component calibration procedures. In this paper, the design and analysis process and the related results are verified through calibration results. The force transducer was designed to fix to rotating hub, and dominant force component was lifting force with maximum 1000 lb. From rotating characteristics, fail-safe structure was required to prevent the rotor from bursting out in case of rotor failure. The sensing element was designed with structural symmetry for self-compensation by full bridge circuit and the expected deformation was analyzed by using finite element method.

1. Introduction

The land-based helicopter testing is required to check the rotor dynamic characteristics and verify load characteristics from design condition. This 6-comonent load cell was developed to measure force and moment occurred at the driving shaft of propeller. From the structural condition of locating at mid-side of rotating shafts, the balance should be made rotationally symmetric in order to minimize unbalance source. At the same time, fail safe structure is required to prevent system failure in case of sensing element failure.

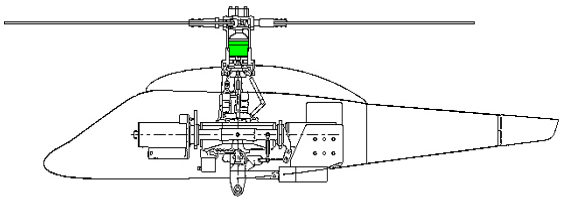

Fig. 1. Location of the 6-component load cell

1.1 Measuring range and characteristics

1) Rated Capacities for Test
Fx: ±100lbs, Fy: ±100lbs, Fz: ±400lbs
Mx: ±500inlbs, My: ±500inlbs, Mz:±1500inlbs
2) Accuracy : 0.5% of Full Load /each comp.
3) Interference : 1.0% of Full Load /each comp.
4) Rated Output: 0.5~2mV/V / each comp.
5) I/O resistance : 350±10 Ω

1.2 Geometry of Sensor

For rotational symmetry, the outer dimension of the load cell has circular ring type which is connected with the inner ring by 4 spokes. The signals for each component of corresponding force and moment are obtained by using the spokes as elastic elements. Driving torque is transferred by spline type coupling machined at the inner bore fitted to engine side by self-locking nut, and the opposite part is linked to rotor blade side by Hub Adapter Shaft with outer rim of the cell, as shown in Fig. 2.

Fig. 2. Sensing element and assembled load cell

2. Design condition

2.1 Materials

Considering material properties like as elasticity, Hysterisis and fatigue, SNCM class 8 was chosen with HRc 45 hardness.

2.2 Fatigue strength

The fatigue strength of the used strain gage, J2A-06-S033P-350, at peak strain ±1700 με is known as 10^6 cycles according to the supplier's report. For guaranteeing infinite life fatigue strength, the maximum tensile strain is limited below 500 με for this design.

3. Strength analysis

Elementary strength analysis was carried out by using beam theory with both ends clamped boundary condition.

3.1 Simple beam model clamped at both ends

Simplified beam model and force and moment distribution is shown in Fig.3 and Fig.4. The shearing force distribution through the beam is $Vx = F$, and the bending moment is calculated as $Mx = \frac{1}{2}FL(1-2\frac{x}{L})$. The maximum bending moment occurs at both ends as $[Mx]_{\max} = \frac{PL}{2}$.

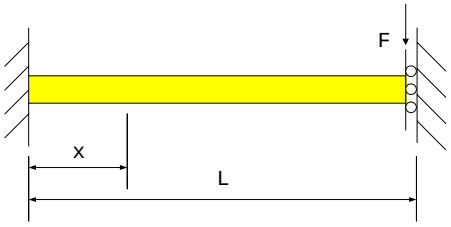

Fig. 3. Both ends clamped beam

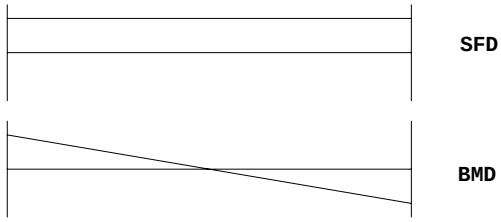

Fig. 4. Shear force and bending moment

3.2 Clamped beam with a hole

A simplified model for clamped beam with holes is shown in Fig.5, which is considered to consist of 3 parts solid center block, clamped ends and hole. In case of loading, it can be assumed that the major portion of deformation occurs at the hole section where is the weakest location. For simplest calculation, the hole section can be assumed to be made of 2 cantilever surrounding the hole at upper and lower sides if the stress concentration effect is negligible dur to the relatively large hole size. In reality, it is sufficient to have analytic solution with this simplified model because the deformation at the weakest point of the hole is major concern.

Using the simplified model, the bending moment at upper surface is $M_I = \frac{1}{8}(2x-L)F$, and the maximum tensile strain is.

$$\varepsilon_I(x) = \frac{-3(2x-L)F}{4Eb(t_o - \sqrt{Lx-x^2})^2}$$

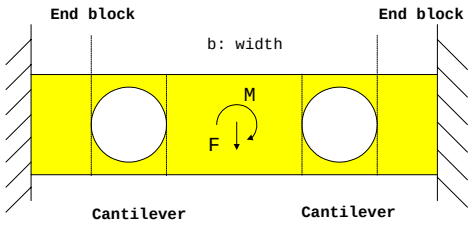

Fig. 5. Clamped beam with holes

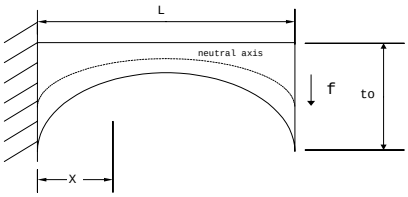

Fig. 6. A simplified beam with a hole

4. Finite element analysis

4.1 Used material properties

1) Young's modulus : $2.1 \cdot 10^{11}$ N/m^2
2) Poisson's ratio : 0.28
3) Shear Modulus : $7.9 \cdot 10^{10}$ N/m^2
4) Mass Density : 7700 Kg
5) Tensile strength : $7.238 \cdot 10^{8}$ N/m^2
6) Yield strength : $6.204 \cdot 10^{8}$ N/m^2

4.2 Boundary Conditions

Since the rotating shaft is linked to outer rim of the load cell through Hub Adapter Shaft, a center point of the spline axis is assigned to be loading point. The other one is another center of spline axis machined at the inner rim of the load cell as axial displacement fixed condition.

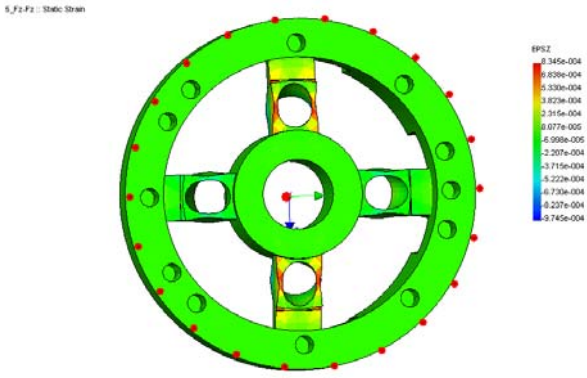

Fig.7. Loading point relative to sensor

4.3 Analyzed results

Numerically calculated stress and strain distributions are shown in Fig. 8 and 9, and the maximum value of stress and strain is shown Table 1.

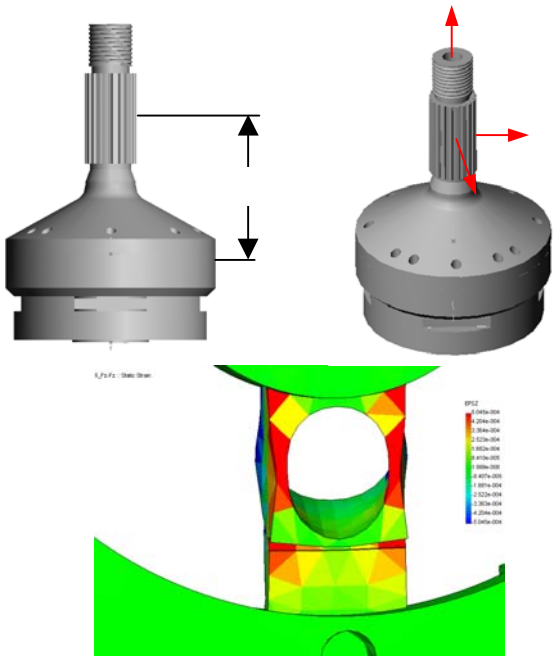

Fig. 8. Tensile strain Ɛxx by Fz

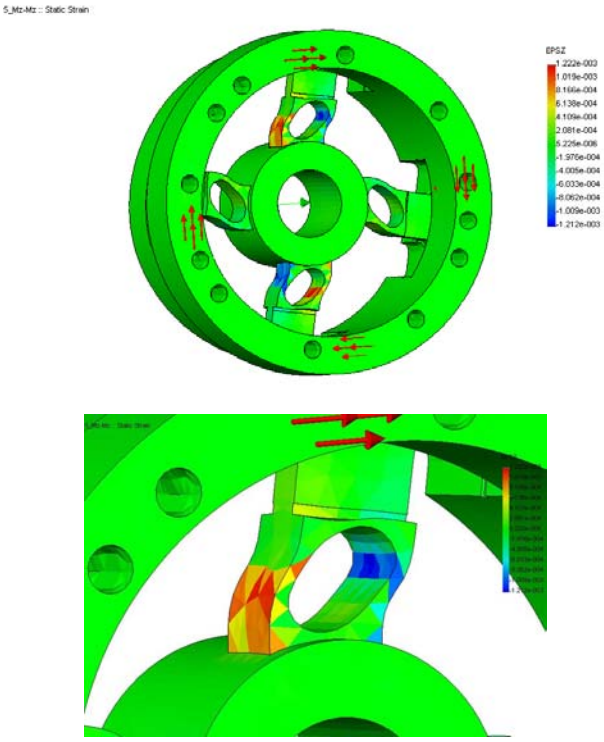

Fig. 9. Tensile strain Ɛxx by Mz

Table 1. Max. stress and strain at a rated load

Mode	σ max (N/m^2)	ε max (μm/m)	Safety Factor
Fx	6.48E+7	186	15
Fy	6.48E+7	186	15
Fz	2.85E+8	420	3.4
Mx	3.30E+8	489	2.95
My	3.30E+8	489	2.95
Mz	3.04E+8	816	3.2

5. Wheastone Bridge circuit

In order to minimize the interference signal between each component, full bridge type electric circuit is used for self-compensation. The gageing positions are shown in Fig. 10.

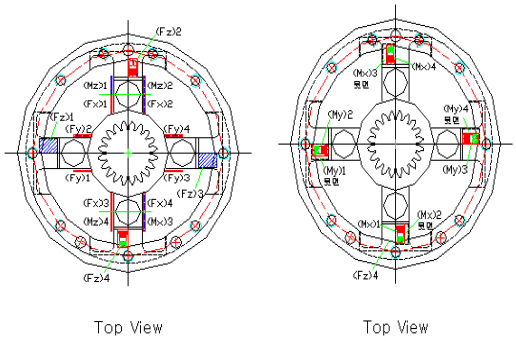

Fig. 10. Strain gage locations for each component

6. Test and Calibration

6.1 Interference reduction

From linear superposition theory of elasticity, the 6-component representing applied load (force and moment) can be expressed as.

$$\{F\} = [C]\{V\} \quad (1)$$

where, {F}: applied load{ Fx, Fy, Fz, Mx, My, Mz },

[C]: 6×6 correlation matrix,

{V} : outpur voltage { V_{Fx}, V_{Fy}, V_{Fz}, V_{Mx}, V_{My}, V_{Mz} }

Using linear algebra, each component of output signal to be measured with respect to applied loading is calculated by multiplying [C*], the inverse matrix of [C], to both sides of eq.(1)

$$\{V\} = [C^*]\{F\} \quad (2)$$

By measuring 6-component output during applying unit load of corresponding component, each element of the inversed compensation matrix [C*] can be obtained as

$$v_j = C^*_{ij} \quad f_i \quad (3)$$

v_j .: j-th output when $f_i \neq 0$ and $f_j = 0 (j \neq i)$

Returning to the eq.(1), the interference reduced result can be obtained by applying compensation matrix to the original signal.

6.2 Multi-component Force Calibrator

For loading of each component except Fz, the specially designed general purpose multi-component force calibrator is used as in Fig. 11. This calibrator was designed as: 1) each component of load is to be applied by using deadweights. 2) multi-component transducer is located at the center of the device with clamping device which can move up and down for leveling. 3) many fitting holes were designed around upper table of the device which can be used to install fixtures like as rollers for deadweight loading.

Fig. 11. Used multi-component force calibrator

6.3 Deadweight type force calibrator for Fz

For loading of Fz, the rated capacity is 400 lb, a deadweight type force calibrator is used with a proper jig as shown in Fig.12.

Fig. 12. Calibration setting for Fz component

6.4 Jig and Fixture for Calibration

The 6-component load cell is located on Base Plate of the calibrator, and the upper plate and a jig for moment arm is assembled, as shown in Fig. 13. The load component for moments, Mx, My, Mz, is applied by applying deadweight through piano wire linked to both ends of moment arm. It is very important to minimize the error terms to be involved during assembly and setting of deadweights, wire, roller and jigs. For excluding unexpected bending effects, rod-end bearings are used at the fitting of wire and jig. In this case, the load range is small, load-induced deflection is not considered

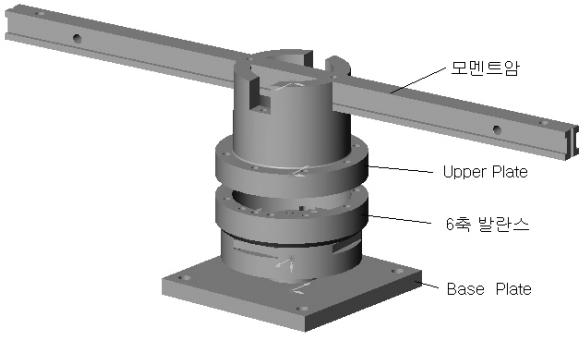

Fig. 13. Assembled calibration jig

6.5 Calibration Software

For automatic measuring and analysis, a Windows based software is developed and used, as shown in Fig. 14.

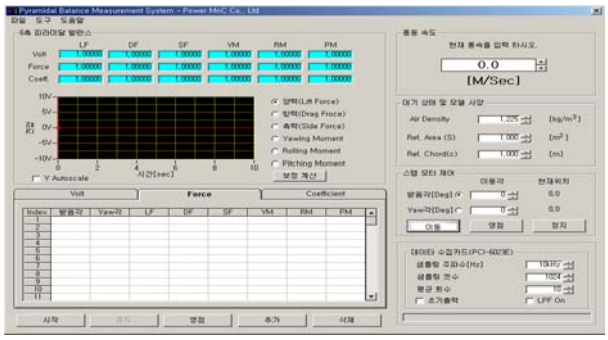

Fig. 14. Automatic calibration software

7. Test results

According to the calibration procedures described in previous article, output signals are measured when the corresponding load component only is applied (that is, the other components are all zero) for each row of Table 2. Using the test results, each elements of the compensation matrix are obtained, as shown in Table 3

Table 2. Output matrix {V} (unit: mV/V for output, Kgf for Force, Kgf*cm for moment)

	V_{Fx}	V_{Fy}	V_{Fz}	V_{Mx}	V_{My}	V_{Mz}
Fx= 40	4.6154 E-01	7.5182 E-02	1.0446 E-02	5.1268 E-02	3.3895 E-01	2.9400 E-03
Fy= 40	1.8460 E-02	4.4072 E-01	4.0260 E-03	3.3553 E-01	6.2616 E-02	4.3140 E-03
Fz= 190	2.4750 E-02	2.2456 E-02	4.1759 E-01	1.5758 E-02	1.1164 E-02	3.9568 E-02
Mx= -600	6.4266 E-02	2.4920 E-03	2.6600 E-03	6.1373 E-01	-1.1110 E-01	1.4558 E-02
My= -600	1.2886 E-02	7.0420 E-02	1.6840 E-02	9.4408 E-02	6.3249 E-01	2.0454 E-02
Mz= 900	1.7786 E-02	2.1030 E-02	3.2300 E-03	6.8640 E-03	1.3680 E-03	4.9909 E-01

Table 3. Compensation matrix [C]

	(Fx)	(Fy)	(Fz)	(Mx)	(My)	(Mz)
(Fx)	-88.34	7.614	1.293	61.56	710.4	57.08
(Fy)	3.398	-90.73	2.624	-744.5	-31.39	-16.32
(Fz)	-4.482	-5.168	-455.5	-75.83	67.31	-168.6
(Mx)	8.686	-2.270	-4.162	-962.8	96.21	-38.48
(My)	-2.958	-9.607	-11.09	62.82	947.6	59.10
(Mz)	3.375	-4.186	-2.972	-47.24	-22.27	-1807

Applying the compensation matrix to output signals, the interference characteristics can be obtained with respect to the normalized diagonal terms, as shown in Table 4.

Table 4. Normalized interference after compensation

	(Fx)	(Fy)	(Fz)	(Mx)	(My)	(Mz)
(Fx)	1	6.595 E-03	2.160 E-03	4.626 E-03	1.997 E-03	2.377 E-03
(Fy)	1.398 E-03	1	1.317 E-03	6.609 E-04	0.000	1.001 E-03
(Fz)	1.398 E-03	1.799 E-03	1	6.609 E-04	1.164 E-03	1.251 E-03
(Mx)	1.998 E-04	5.995 E-03	2.002 E-03	1	3.727 E-03	3.603 E-03
(My)	4.395 E-03	1.199 E-03	6.848 E-04	8.642 E-03	1	3.786 E-03
(Mz)	8.190 E-03	4.396 E-03	1.317 E-03	1.322 E-03	5.657 E-03	1

8. Conclusion

A 6-component force transducer was successfully developed and evaluated for land-based rotor dynamic test of helicopter with fail-safe structural design.

Contact Point: Jae-Young JEON, Ph.D.
R &D Center, POWER MnC Co., Ltd.
461-36, Chunmin-dong, Yusong-gu, Taejon, KOREA
tel: +82-42-527-5920
fax: +82-42-523-9910
e-mail: pw@powermnc.com
Web-page: www.powermnc.com